Diurnal and Tidal Variation of Temperature and Salinity in the Ponta Rasa Mangrove Swamp, Mozambique

4 authors, including:

Antonio Mubango Hoguane
Eduardo Mondlane University
25 PUBLICATIONS 153 CITATIONS

SEE PROFILE

John H. Simpson
Bangor University
176 PUBLICATIONS 7,158 CITATIONS

SEE PROFILE

D. G. Bowers
Bangor University
81 PUBLICATIONS 2,291 CITATIONS

SEE PROFILE

Some of the authors of this publication are also working on these related projects:

Project

Capacity building for sustainable Fisheries Management in the Southwest Indian Ocean region - FisherMan View project

Diurnal and Tidal Variation of Temperature and Salinity in the Ponta Rasa Mangrove Swamp, Mozambique

A. M. Hoguane[a], A. E. Hill[b,c], J. H. Simpson[b] and D. G. Bowers[b]

[a]*Instituto de Investigação Pesqueira, P.O. Box 4603, Maputo, Mozambique*
[b]*University of Wales, Bangor, School of Ocean Sciences, Menai Bridge, Gwynedd LL59 5EY, U.K.*
[c]*NERC Centre for Coastal and Marine Sciences, Proudman Oceanographic Laboratory, Bidston Hill, Prenton, U.K.*

Measurements of hydrographic conditions in the Ponta Rasa tidal mangrove swamp, Inhaca Island, Mozambique were made in August–October 1994 during the winter dry season. The Ponta Rasa swamp/creek is tidally choked on account of the narrow channel that connects it to Maputo Bay and at neap tides, a sill prevents bay water entering the creek system altogether. Temperature variation in the swamp (15–25 °C) was predominantly diurnal with an additional signal due to the tidal advection of bay waters. There is no river discharge into Ponta Rasa and during the observation period, there was no significant rainfall. The mean salinity in the swamp (*c*. 38) was controlled by evaporation and transpiration by mangroves and an overall evapotranspiration rate of 0·5 cm day^{-1} was estimated from a steady salt balance. Salinity variation (*c*. 2) was predominantly due to semi-diurnal tidal advection of lower salinity Maputo Bay water into the swamp/creek. A model which incorporates tidal dynamics coupled to heat and salt balance equations reproduces many of the observed features of the system.   © 1999 Academic Press

Keywords: tides; temperature; salinity; evapotranspiration; sill; mangrove swamps; Mozambique

Introduction

Mangrove swamps are an important component of tropical ecosystems; they help protect coastlines from erosion and provide important artisanal fisheries to local communities (Vance *et al.*, 1990). However, these systems are under stress from both human activities (e.g. urbanization, water quality, mangrove exploitation) and natural processes (sedimentation, excessive temperature fluctuations and high salinities). For example, Gundry *et al.* (1981) point out that although salt is important for growth and survival of mangrove plants, extreme high salinity (over 40) would retard even the most resistant species. It is, therefore, of importance to examine the factors which regulate the temperature and salinity in mangrove swamps. The Ponta Rasa and Saco de Inhaca mangrove swamps on Inhaca Island, Mozambique (Figure 1) are particularly notable because no rivers drain into them and during the austral winter, when seasonal rainfall is low, salinity can become as high as 42 (Macnae & Kalk, 1969).

In this paper observations are reported from the Ponta Rasa mangrove swamp in the dry season and with the assistance of a coupled hydrodynamic–thermodynamics model, the mechanisms responsible for regulation of temperature and salinity fluctuations in the system are examined.

The study site

The Ponta Rasa mangrove swamp is located in the south-western part of Inhaca island (26°S) on the eastern side of Maputo Bay [Figure 1(a)]. The island forms part of the barrier which protects Maputo Bay from the open ocean and is 11 km long and 6 km wide. Tides in Maputo Bay are predominantly semi-diurnal with a range of *c*. 2 m at springs [Table 1; Figure 3(a)]. A single narrow channel connects Maputo Bay and the Ponta Rasa creek [Figure 1(b)]. The creek is 500 m long, 3 m wide and has an average depth of 1 m at low water. The creek is surrounded by tidal flats (the swamp) which are about 2 km long with an average width of 100 m [Figure 1(b)]. The total area of the swamp is 0·2 km², of which 70% is covered by mangrove vegetation. The Ponta Rasa swamp is tidally flooded twice a day, at spring tides, through the channel and the tidal range within the creek is *c*. 1 m. The creek is located about 0·6 m above the mean sea
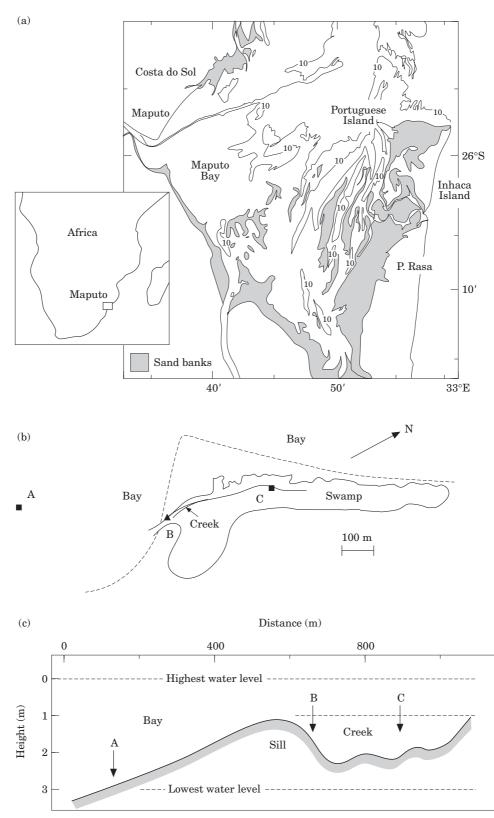
(a)

(b)

(c)

FIGURE 1. (a) Location of Maputo Bay, (b) plan view of the Ponta Rasa mangrove swamp, (c) longitudinal section along the Ponta Rasa creek.

TABLE 1. Tidal constituents in Maputo Bay

Constituent	Amplitudes (metres)				Phase (degrees, Greenwich)			
	MH	CS	PR	PI	MH	CS	PR	PI
M_2	0·94	0·93	0·856	0·820	123	113·5	110·4	109·8
S_2	0·55	0·54	0·558	0·460	164	156·5	150·9	149·0
N_2	0·16	0·14	0·151	0·128	110	108·0	103·3	110·5
K_1	0·04	0·04	0·032	0·036	201	187·3	180·9	176·7
O_1	0·03	0·03	0·031	0·020	1·5	349·3	334·0	330·0
M_4	0·01	0·01	0·021	0·02	164	173·0	213·7	211·0

MH, Maputo Harbour; CS, Costa do sol; PI, Portuguese Island; PR, Ponta Rasa.

level, but it does not dry out completely at low water because there is a sand barrier (sill) at the outlet to the bay which prevents creek water from draining out to sea [Figure 1(c)]. The sill also prevents water entering the creek until late in the flood tide and, during neap tides, there is no flow of water into the channel. The swamp around the margins of the creek dries out at low water, except for small pools which retain some water. There is no river input to the swamp and although there is evidence of fresh ground water (Macnae & Kalk, 1969), rainfall is the main source of fresh water to the system.

Methods

Field measurements comprising tidal elevation, water velocity, water temperature and salinity were made in the Ponta Rasa mangrove swamp from 20 August to 5 October (year days 232–267), 1994. The measurements were made using Aanderaa RCM7 current meters and Aanderaa WLR4 water level records equipped with temperature and conductivity sensors from which salinity was computed (throughout this paper salinity is expressed as values on the practical salinity scale (UNESCO, 1978). Water speed was measured with a precision of 0·01 m s^{-1} and temperature, salinity and pressure were measured with an accuracy of ±0·10 °C, 0·03 and 0·001 decibar respectively. Data were recorded every 10 min.

The instruments were moored at three locations [Figure 1(b)]. Temperature and salinity were measured at all sites. In the bay adjacent to the mouth of the creek (site A) and in the middle of the creek (site C), tidal elevations were measured. In the connecting channel between the bay and the swamp/creek (site B), current speeds were measured but no elevations were recorded. Instruments were deployed at low water and were tied to poles fixed into the ground. The water level recorders were levelled in relation to a

temporary bench mark. In some cases, particularly during neap tides, the instruments were exposed to the atmosphere and so recorded air temperature and atmospheric pressure. The current meters recorded water speed only at a fixed height (0·4 m) above the bed. Since the flow in the channel was mainly bi-directional, the direction of the flow was determined using water level data and the velocity was set positive (negative) in the directions into (out) of the swamp. The cross-sectional average velocity was then estimated assuming a vertical logarithmic velocity profile and the Chezy formula using the method of Turrell et al. (1996). Velocity records obtained in this way were, however, limited because floating debris that swept out of the creek, particularly during spring tides often fouled the rotors.

Meteorological data consisting of hourly records of air temperature, atmospheric pressure at mean sea level and daily precipitation at Maputo City were obtained from the National Meteorological Centre, Maputo (Figure 2). The atmospheric pressure records were used to correct the Aanderaa water level recorders for the inverse barometer effect. Aerial photography was used to map the area of the swamp and estimate the total area covered with vegetation.

Results

Tides

The tides in the Maputo Bay near Ponta Rasa (site A) were predominantly semi-diurnal [Figure 3(a)]. The sum of O_1 and K_1 tidal constituent amplitudes is less than 5% of that of the sum of M_2 and S_2. The measured tidal range was about 2 m at spring tides. The results of harmonic analyses of the data are consistent with predictions from tide tables for Portuguese Island at the entrance of Maputo Bay about 10 km north of Ponta Rasa and with the tides
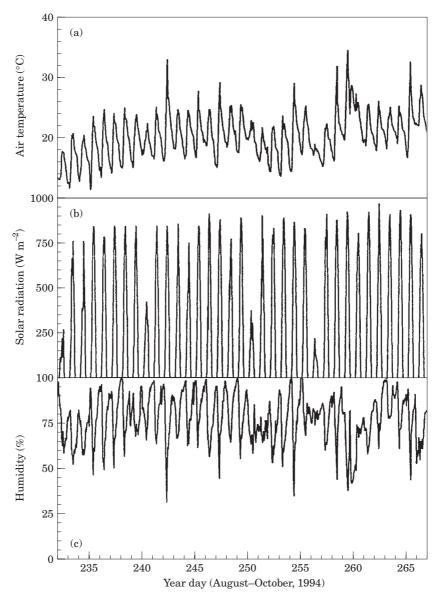
FIGURE 2. (a) Air temperature, (b) solar radiation, (c) relative humidity at Maputo meteorological station during the observation period 20 August–5 October 1994.

measured in Maputo Harbour (Anon, 1993 and Table 1). In the connecting channel between the bay and the creek (site B), the limited current measurements indicated flow speeds up to 0·8 m s^{-1} [Figure 4(a)]. In the Ponta Rasa creek at site C [Figure 5(a)], tidal amplitudes were much smaller (0·8 m at springs) and were typical of tides in a choked lagoon with lowest water levels occurring at neap rather than spring tides (e.g. Hill, 1994). At site C, the main flood and ebb periods were both short (<2 h) but after the main ebb there was a longer period (>4 h) of slow drainage of the creek. This feature of the tidal curve is apparent in Figure 6(a) which shows an expanded

segment of the record in Figure 5(a). The short flood tide duration occurred because the sill, which was about 0·5 m above the mean sea level, prevented water entering Ponta Rasa swamp during the early phase of the flood tide. During each neap tide, when the bay tidal range is small (<0·6 m), water did not enter the creek at all for about a three day period [Figure 5(a)].

Temperature

The water temperature time series [Figures 3(b), 4(b) and 5(b)] exhibited a similar pattern to that of air
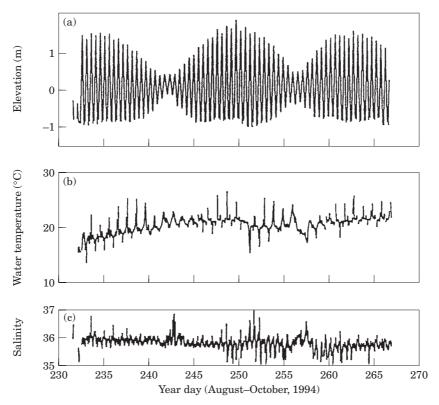
FIGURE 3. (a) Surface elevation, (b) water temperature, (c) salinity at site A in Maputo Bay near to the Ponta Rasa entrance channel.

temperature [Figure 2(a)]. The mean water temperatures in the creek showed an overall warming trend from 15 °C to 21 °C which matched the air temperature trend. Similarly, both air and water temperatures showed marked diurnal signals which were in phase. Highest temperatures were attained at approximately 18:00h local time and lowest temperatures at approximately 06:00h [e.g. Figure 6(b)]. Tidal influence was also present in the water temperature records. This can be seen, for example, by the sudden drops (c. 2 °C) in the water temperature on the nocturnal flood tides. This occurred because as bay water rose in a shallow layer over the beach face (seaward of the sill) it was cooled in contrast to the deeper (c. 1 m) water in the creek on the swamp side of the sill. There is also an indication that, during day-time flood tides, there was a slight temperature increase as bay water was heated by the sun as it formed a shallow layer over the sandy beach-face before it entered the creek [Figure 6(b)]. During summer the latter effect is much more pronounced with temperature step-increases on daytime flood tides of c. 3–5 °C (Hoguane, 1996). In any event, the magnitude of the flood temperature step-increase varies according to the time of the day (and cloud cover) and is greatest for flood tides which occur in the early afternoon (Hoguane, 1996).

The diurnal temperature amplitudes of the water in the bay [site A, Figure 3(b)] were small (c. 2 °C) compared to those observed in the creek (c. 5 °C) at sites B and C [Figure 4(b), 5(b)]. The spikes in the water temperature observed at site A in the bay [Figure 3(b)], were the result of exposure of the instruments to the air during low water. The temperature amplitudes of the water at the mouth of the creek [site B, Figure 4(a)] were slightly larger compared with those of water in the middle of the creek [site C, Figure 5(a)], probably because site B was exposed to incoming solar radiation whereas site C was shaded by vegetation.

Salinity

In contrast to the temperature signal which was predominantly diurnal, the salinity signal showed a marked semi-diurnal tidal influence [Figure 6(b,c)]. The salinity in the bay showed a small amplitude (<0·5) tidal variation about a mean salinity of c. 36 [Figure 3(c)]. Apart from at neaps, on each flood tide the salinity in the creek (sites B and C) dropped to the bay value (35–36) and increased again as the tide fell to attain a maximum (37–40) at low water [Figures 4(c), 5(c), 6(c)]. The amplitudes of the salinity
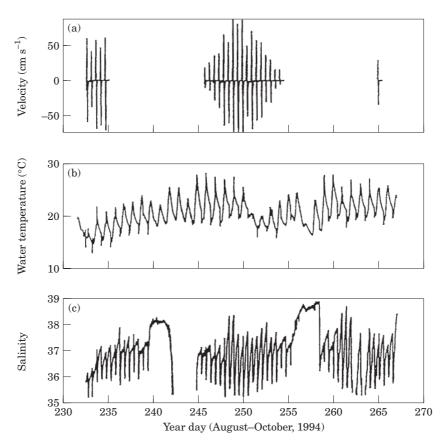
FIGURE 4. (a) Water velocity, (b) water temperature, (c) salinity at site B in the channel connecting the Ponta Rasa creek to Maputo Bay.

fluctuations increased with the distance away from the channel entrance and at times of increased tidal range near spring tides, suggesting the presence of a longitudinal salinity gradient down the creek.

As mentioned previously, at low tides, water was left trapped in extensive pools within the swamp region. Surveys in June–July 1995 showed salinity in the pools varied from 40 to 43 in deeper pools (about 2 cm deep) to 49 in shallow pools (1 cm deep). Salinity in the sediments ranged from 44 up to 52 (Hoguane, 1996). Higher values were obtained in the deep sediments (5 cm below the ground). The differences in salinity between the water in pools and that in the sediments were on average about four. There was no evidence of a spatial gradient of salinity of the swamp. During the three days around neap tides, when there was no advection of water into the creek (due to the sill), the salinity within the creek [e.g. site C, Figure 5(c)] showed no tidal variation. Instead the creek salinity showed a small, but steady, increase of *c*. 1–2, probably due to the effect of evapotranspiration and the outwelling of saline water from saline pools in the swamp.

Evapotranspiration

Evapotranspiration was computed from an assumed steady state mass balance within the swamp. It is assumed that the net volume flux (averaged over a tidal cycle), Q_R, into the swamp (through the channel) balances that lost by net evaporation from the surface of the swamp, i.e.

$$Q_R = A_s(E - P) \tag{1}$$

where E is the evapotranspiration rate, P is the precipitation rate, and A_s is the flooded surface area of the swamp. Following Simpson *et al.* (1996), an independent estimate of Q_R can be found by assuming that the net flux of salt out of the channel per tidal cycle (due to the tidal salt pumping) is balanced by a compensating residual flux of salt into the swamp, i.e.

$$\bar{Q}_R = -\left[\frac{\overline{(<Q> - Q)\,(<S> - S)}}{<S>} \right] \tag{2}$$

where, Q and S are respectively the instantaneous tidal volume flux and instantaneous salinity obtained
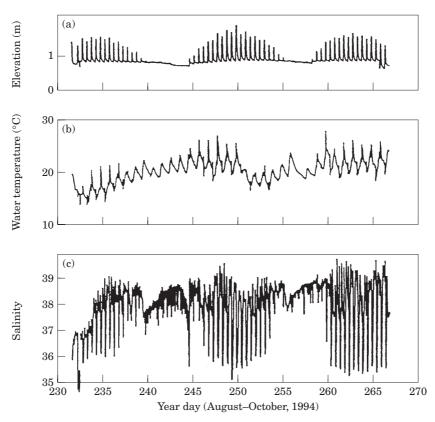
FIGURE 5. (a) Surface elevation, (b) water temperature, (c) salinity at site C in the Ponta Rasa creek.

from measured values at site B. Here < > indicates an average over one tidal cycle and overbars indicate an ensemble average of many tidally-averaged quantities. In Ponta Rasa the average surface area of the swamp was $A_s = 8 \times 10^4$ m^2, $P = 0$ and the residual volume flux was estimated from Equation (2) as $Q_R = 0.004$ m^3 s^{-1}, with an uncertainty of 0.001 m^3 s^{-1}. The range of values of this important figure is mainly due to the uncertainty in measuring cross-sectional areas and velocities. Equating (1) and (2) above, the overall evapotranspiration rate was estimated to be $E = 0.5$ cm day^{-1} which is consistent with estimates from other mangrove systems (e.g. Mazda et al., 1990; Wattayakorn et al., 1990; Table 2). By comparing this figure with evaporation estimates from the tidal swamp at Costa do Sol which contains no mangroves [Figure 1(a)], Hoguane (1996) has estimated that evapotranspiration is partitioned between evaporation and mangrove transpiration in the ratio 3:2 respectively.

Flushing time

If the flushing of the creek is assumed to be due to tidal diffusion, the longitudinal tidal diffusion coefficient, B (m^2 s^{-1}) can be estimated using the lateral

trapping method developed by Wolanski and Ridd (1986),

$$B = (K/(1+\varepsilon)) + (\varepsilon u^2 a^2 \tau)/(48(1+\varepsilon)) \qquad (3)$$

where K is the along channel eddy diffusivity, u is the characteristic water velocity, ε is the ratio of the swamp volume to the creek volume, $a = T/\tau$ is the fraction of tidal cycle when the swamp is immersed where τ and T are the tidal period and the period for which the swamp is immersed, respectively. In Ponta Rasa it was estimated that $\varepsilon = 8$, $u = 0.5$ m s^{-1}, $T = 2$ h, $a = 1/6$, hence the diffusion coefficient was estimated as $B = 5.4$ m^2 s^{-1}. The flushing time $\tau_o = l^2/B$ (Wattayakorn et al., 1990; Wolanski et al., 1990) was estimated to be $\tau_o = 14$ h, assuming that the length of the creek is $l = 500$ m. This implies that, during spring tides, the swamp may be flushed in a single tidal cycle. During the neap tides, however, when only a small amount of water from the bay enters the creek, complete flushing of the swamp may take up to five days.

A hydrodynamic–thermodynamic model for Ponta Rasa

In order to further explore the variability in the Ponta Rasa system, a mathematical model has been
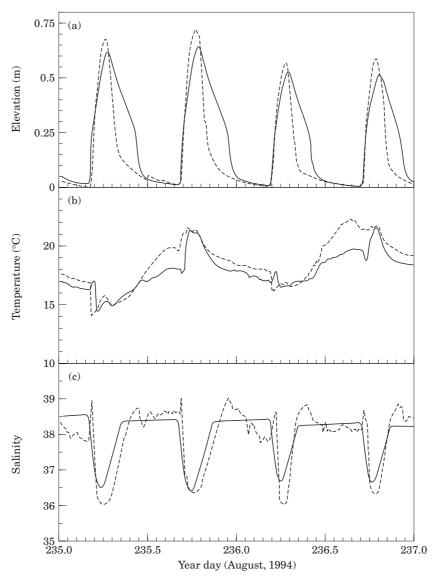
FIGURE 6. Expanded time series of (a) surface elevation, (b) water temperature, (a) salinity at site C in the Ponta Rasa creek. Observations: dashed line; model: solid line.

developed. The purpose is to investigate quantitatively to what extent the observed variability can be accounted for using a model which incorporates only the minimum of governing physics (tides, surface heat and salt fluxes). There are relatively few hydrodynamic models describing mangrove swamp systems. Wolanski *et al.* (1980) and Ridd *et al.* (1990) have used one-dimensional channel models but these are probably over-complex for this case since the Ponta Rasa creek is short and hence tidal phase propagation is unlikely to be important. Simpson *et al.* (1996), on the other hand, used a box model approach for salt budget calculations but this contains no dynamics and cannot address issues relating to variability on

tidal time-scales. In this paper, therefore, an intermediate class of model is adopted which contains the minimum of dynamics required to reproduce the tides in the swamp but thereafter treats the swamp as a filling box. Coupled to the dynamic model are two conservation equations for heat and salt in the swamp.

The dynamical model

The Ponta Rasa system can be regarded as made up of two-reservoirs (Figure 7). In the first reservoir (the bay), tidal elevations, temperatures and salinities are prescribed. The second reservoir (the swamp)

TABLE 2. Evapotranspiration rate as estimated in different mangrove swamps

Mangrove swamp	Evapotranspiration cm day^{-1}
Klongo Ngao, Thailand[1]	0·5
Coral Creek, Australia[2]	0·5
Bashinta-Minato, Japan[3]	0·71
Ponta Rasa, Mozambique[4]	0·5

These results were obtained from [1]Wattayakorn et al., 1990; [2]Ridd et al., 1990; [3]Mazda et al., 1990; [4]this study.

responds to the bay forcing as a filling box. The swamp is connected to the bay by a narrow, short frictional channel, at the entrance of which is a shallow sill. All the relevant creek dynamics are assumed to be confined to this channel. Direct wind stress is neglected, on account of the dense vegetation. Following Hill (1994) the equation of motion in the channel, neglecting the inertial term, is

$$g(\eta_s - \eta_b)/L = -ku|u|/(H - \eta_m) \quad (4)$$

and the mass conservation equation for the swamp is

$$A(\eta^\star)(d\eta_s/dt) = -w(\eta_m - H)u \quad (5)$$

In the above, u is the cross-sectionally averaged water velocity in the channel, set positive inwards, k is the friction coefficient, η_s and η_b are the swamp and bay surface elevations, respectively, measured relative to the bay mean sea level. The length and width of the connecting channel are L and w respectively. The height of the sill above bay mean sea level is H (Figure 7). The mean elevation in the channel is $\eta_m = (\eta_s + \eta_b)/2$. Flooding of the swamp is only permitted to take place when the water level in the bay reaches that of the prescribed sill level, thus the sill delays and shortens the flooding period of the swamp. The flooded swamp surface area is $A(\eta_\star)$ which was estimated by the hyposometric relationship derived by Simpson et al. (1996), namely

$$A(\eta^\star) = \varphi\eta^\star - a \quad (6)$$

where φ (m) is a coefficient of regression between the observed discharge and the observed rate of change of the water elevations in the swamp, a is a coefficient and $\eta_\star$ is the elevation (m) above the sill ($\eta^\star = \eta_m - H$ in Figure 7). In Ponta Rasa $\varphi = 1\cdot28 \times 10^5$ and $a = 2\cdot58 \times 10^4$. The equation fits the observations with $r^2 = 0\cdot86$.

Solving Equation (4) for velocity and substituting into (5) a single, non-linear expression is obtained for elevation η_s in the swamp

$$d\eta_s/dt = \sqrt{(w^2 g(\eta_m - H)^3/kLA^2(\eta^\star))} \cdot$$
$$((\eta_b - \eta_s)/\sqrt{(|\eta_b - \eta_s|)} \quad (7)$$

Using this relation, η_s can be determined by integrating forward over time from an initial condition of zero elevation everywhere and with prescribed tidal forcing in the bay, η_b. The velocity in the channel is then computed from the continuity Equation (5), and is given by,

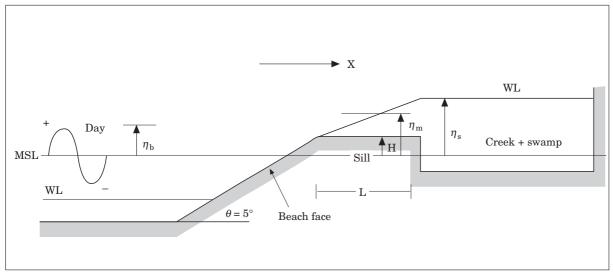$$u = (A(\eta^\star)/(w(\eta_{m-H)) \cdot d\eta_s}/dt \quad (8)$$

FIGURE 7. Definition sketch of the Ponta Rasa system. See text for definition of symbols.

The features of Equation (7) are discussed at length by Hill (1994). Briefly, the water elevation in the swamp is controlled by the geometry of the system, friction and the tides in the bay. The system is tidally choked and hence the elevation amplitude in the swamp decreases with increasing friction, length of the channel and swamp area and swamp elevation increases with increasing width and depth of the channel.

The thermodynamic model

The temperature and salinity in the mangrove swamp in Ponta Rasa was computed by considering the advection of water between the bay and the swamp through the connecting channel and allowing vertical exchange of properties with the atmosphere within the swamp. The equations for temperature and salinity in the swamp are respectively,

$$dT_s/dt = A_c u(T_b - T_s)/V + Q_N/(\rho c_p h_s) \qquad (9)$$

and

$$dS_S/dt = A_c u(S_b - S_s) + (E - P)S_s/h_s. \qquad (10)$$

The continuity equation is

$$dV/dt = A_c u - (E - P)A_L \qquad (11)$$

where V is the total volume of water within the swamp, A_c is the cross-sectional area of the channel and the average water depth in the swamp is h_s. A_L is the surface area of the lagoon. The evapotranspiration and precipitation rates are E and P respectively, c_p is the specific heat of the water, ρ is the water density and T and S are the temperature and salinity respectively. As before, the subscripts s and b refer to the swamp and bay respectively. The net heat flux through the water surface (the balance between solar radiation, long wave radiation, evaporative and sensible heat losses) is Q_N and this is assumed to be readily mixed through the water column. This assumption is supported by longitudinal sections of temperature and salinity in the creek (Hoguane, 1996). The coupling between the dynamical model (Equation 7) and the above heat and salt Equations (9 and 10) occurs because of the tidal advection velocity, u, in Equations (9) and (10) and because the changing swamp water level, η_s, alters the volume, V, of the swamp and the average water depth, h_s both of which appear in the denominators of Equations 9 and 10.

During the ebb, the salinity in the lagoon does not depend on the salinity in the open sea. Therefore during the ebb, the term $S_b - S_s$ vanishes, and the salinity within the lagoon depends only on the evapotranspiration term.

The overall evapotranspiration rate, E, in the swamp was held constant at 0.5 cm day^{-1} (or 0.25 cm per tidal cycle), based on the calculation set out previously. Evapotranspiration was assumed to take place only during the time when the swamp was inundated (2 h during each tidal cycle). The assumption of constant evapotranspiration can be justified if it is considered that some portion of water is left in the pools and in the sediments in each tidal cycle to evaporate and uptake by plants, leaving salt behind. During each inundation, the incoming water will directly evaporate or be taken up by plants and it will leach the salt left behind by the previous tide. For the flood occurring in the night there will be no direct freshwater uptake by the plants, because the stomata close in the dark (Coulter, 1973; Roberts *et al.*, 1990; 1993), but there will be leaching out of the salt left behind during the last flood, which should have occurred during the daytime. For the flood occurring during the daytime, there will be no salt left in the swamp for leaching because the previous flood occurred during the night, but there will be direct freshwater uptake by the plants. It seems, however, that the salt left behind on the swamp and that due to direct freshwater uptake by plants have the same order of magnitude.

Model parameters and boundary conditions

Equation (7) was solved numerically for elevation in the lagoon using a fourth-order Runge-Kutta method. The elevation in the bay, η_b was prescribed as a sum of six tidal constituents based on a harmonic analysis of the record in Figure 3(a) (column labelled PR in Table 1). The model time-step was set to 5 min. The flooded area at each time step was estimated using the hypsometric relationship in Equation (6), using the elevation calculated on the previous time-step. The length of the channel, L, was taken to be 85 m and its width, w, as 15 m and sill height $H = 0.6$ m. The friction coefficient was set to a constant value, $k = 0.05$, a value which provides a friction force comparable with that obtained by Wolanski *et al.* (1992) using Manning's roughness coefficient.

The right hand side of the temperature and salinity Equations (9) and (10) comprises two terms. The first term on the right hand side of each represents advection of bay water properties into the swamp, the second term includes the local meteorological forcing (net heating term for the temperature equation and the evapotranspiration and precipitation term for
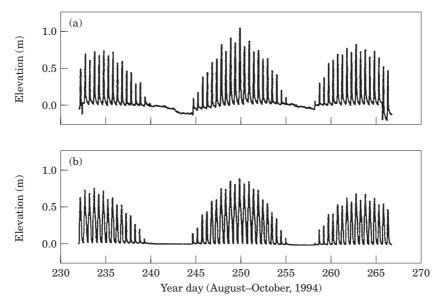
FIGURE 8. Surface elevation (m) in the creek in Ponta Rasa, (a) observed, (b) and modelled.

salinity equation). The bay temperature and salinity values were prescribed to the model from the time series at site A, filtered to remove the spikes due to drying of the instruments [Figure 3(b) and (c)]. Additionally a beach compartment was introduced to the model in order to incorporate the effect of warming or cooling of bay waters as they rose over the beach-face prior to entry to the channel (Figure 7). The beach face was divided into three boxes and water heated (or cooled) by exchange of heat within the atmosphere in each of these compartments as the bay water level rose towards the sill.

At the surface, the model was forced by the observed solar radiation and air temperature for Maputo (Figure 2). The net heat flux, Q_N, was computed using the formulae of Gill (1982), corrected for the effect of the vegetation by the Beer–Lambert formulae (Roberts *et al.*, 1993). Relative humidity and wind speed were set to constant values of 75% and 5 m s^{-1}, respectively (average of daily observations taken during the observing period), and the vegetation albedo was set to 15%, representative of the conditions in Ponta Rasa (Hoguane, 1996). The temperature and salinity equations were also integrated forward with a 5 min time-step.

Model results

The model reproduced the tidal elevations in the swamp reasonably well (Figure 8) and a regression analysis of the observed against computed elevations yielded $R^2 \approx 0.78$. The model did not reproduce the variation over the springs-neap cycle of the elevation set-up in the swamp which may have been because of uncertainty in determining the height of the sill.

Only a few good quality velocity observations were obtained but the model results were in fair agreement with these (Figure 9). However, at spring tides, the model underestimated the velocity at high water and overestimated it at low water. This may be due to the error in estimating the friction and also due to the broad assumption of a rectangular cross-section basin.

The modelled swamp temperatures (Figure 10) show a marked diurnal oscillation, due to diurnal variations in the solar radiation. The steep drops in temperature during the flood tides at night are also reproduced on account of the inclusion of the beach compartment in the model. The model fits the observations at site C better than at site B, probably because the instruments at site B were placed in the open, exposed to higher solar radiation, as mentioned previously. The regression between the observed and computed temperatures yielded a slope 1 and $R^2 = 0.06$, for the observations at the channel entrance (site B). For the observations near the head of the creek (site C) the regression slope was 1 and $R^2 = 0.72$, the main source of error lies in the estimate of the volume fluxes through the channel. This includes the limitations in the hydrodynamics, discussed earlier and in the determination of the geometry of the channel. The width of the channel was set to a constant value whereas in reality it increases with water height. This simplification leads to an
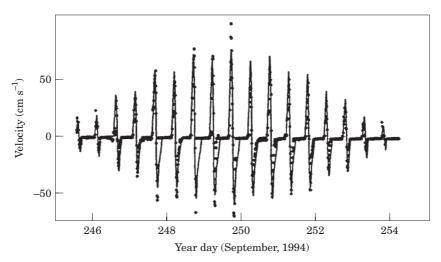
FIGURE 9. Water velocity in the Ponta Rasa entrance channel, observations (solid points), modelled (solid line).
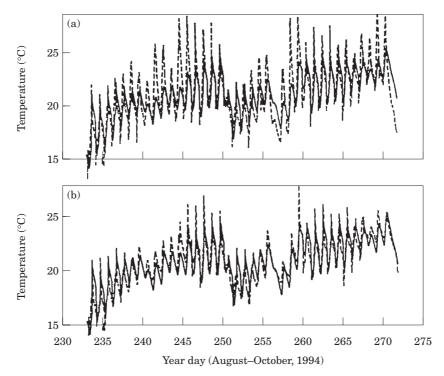

FIGURE 10. Water temperature in the Ponta Rasa creek at (a) site B and (b) site C. Observed (dashed line) and modelled (continuous line).

underestimation of the water inflowing during higher water and during spring tides and to an overestimation during low water and during neap tides.

The salinity model reproduced the tidal fluctuations reasonably well (Figure 11). The regression analysis of the average salinity in the low and high water yielded 0·8 for the slope and $R^2 = 0·6$. The main limitation of the salinity model lies in the fact that complete mix-ing, upon which it is based, does not hold and there is a longitudinal salinity gradient (*c.* 3 per 500 m) down the creek.

Discussion and conclusions

This paper has reported detailed measurements of the hydrodynamic regime, temperature and salinity
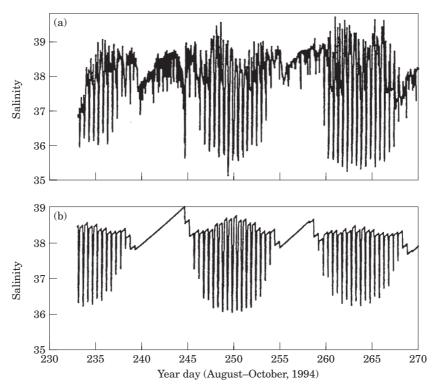
FIGURE 11. Salinity in the Ponta Rasa creek at site C, (a) observed, (b) modelled.

in a mangrove swamp and shown how they can be interpreted using a simple physical model.

Similar hydrodynamic and thermohaline models has been applied to other lagoons and estuaries elsewhere in the world (Stigebrandt, 1980; De Silvo & Fiorillo, 1981; Van de Kreek, 1990; Hill, 1994). The novel feature here is the application of this type of model to a mangrove lagoon. In order to achieve agreement with observations in the lagoon, two important modifications have had to be carried out. The first of these was increasing the bottom friction coefficient to $k=0.05$. This is a factor of 20 times greater than that used in most estuarine models and reflects the fact that mangrove trees and particularly their root systems, represent highly frictional bodies to water movement. The second change, which was necessary to allow modelling of temperature and salinity in the lagoon water, was to allow the water surface to vary with water elevation in the lagoon.

The resulting model is relatively simple, and it has been deliberately kept so in order to reduce the number of free variables. As a consequence, the model can be easily applied to other mangrove systems. Other models of mangrove systems (Wolanski et al., 1980) are relatively detailed and require good knowledge of the topography of the creek and swamp.

The model has confirmed that the hydrodynamics of the mangrove lagoon are controlled by the tides in the bay, friction by the mangrove trees and the geometry of the connecting channel (Wolanski et al., 1990; Mazda, 1990; Hill, 1994). In particular, in a silled lagoon, such as Ponta Rasa, the height of the sill is critical. A high sill restricts the amount of water entering the lagoon on the flood tide and increases the flushing time. There are further implications for water temperature. During the flood, shallow water is held on the beach, where it is heated (during daytime) and cooled (during the night) before entering the lagoon, thus increasing the diurnal temperature amplitude in the lagoon, with consequences for the biology and chemistry.

There are many mangrove systems in the world that are similar to Ponta Rasa and to which the model that has been described here can be readily applied. Typical examples are Bashita-Minato in Japan, Coral Creek in Australia and the Hacuraca Experimental mangrove forest in Brazil.

References

Anon 1993 *Admiralty tide tables and tidal stream tables*. Vol. 2. Hydrographer of the Navy.

Coulter, D. J. 1973 Prediction of evapotranspiration from climatological data. *Proceedings of the Soil and Plan Water Symposium, DSIR Information Series* **96,** 38–45.

De Silvo, P. H. & Fiorillo, P. 1981 Modelling of lagoons: the experience of Venice. In *Transport Models for Inland and Coastal Waters* (Fischer, E. B., ed.). Academic Press, New York, pp. 112–139.

Gill, A. E. 1982 *Atmospheric–ocean dynamics.* Academic Press, New York, 662 pp.

Gundry, J. M., Drennan, M. & Bejark, P. 1981 Salinity control in relation to pre-abscission propagule development in *Avicennia marina* (Forsk) Verh. *Electronic Microscopy Society of South Africa—Proceedings* **11,** 155–156.

Hill, A. E. 1994 Fortnightly tides in a lagoon with variable choking. *Estuarine, Coastal and Shelf Science* **38,** 423–434.

Hoguane, A. M. 1996 *Hydrodynamics, Temperature and Salinity in Mangrove Swamps in Mozambique.* Ph.D. Thesis, University of Wales, Bangor.

Macnae, W. & Kalk, M. 1969 *A natural history of Inhaca Island, Mozambique.* Witwatersrand University Press, 174 pp.

Mazda, Y., Sato, Y, Sawamoto, S., Yokochi, H. & Wolanski, E. 1990 Links between physical, chemical and biological processes Bashita-Minato, a mangrove swamp in Japan. *Estuarine, Coastal and Shelf Science* **31,** 817–833.

Ridd, P., Wolanski, E. & Mazda, Y. 1990 Longitudinal diffusion in mangrove-fringed tidal creeks. *Estuarine, Coastal and Shelf Science* **31,** 541–554.

Roberts, J., Cabral, O. M. R. & de Aguiar, L. F. 1990 Stomatal and boundary layer conductances in an Amazonian terra firme rain forest. *Journal of Applied Ecology* **27,** 336–353.

Roberts, J., Cabral, O. M. R., Fish, G., Molin, L. C. B. & Moore, C. J. 1993 Transpiration from an Amazonian rainforest calculated from stomatal conductance measurements. *Agriculture and Forest Meteorology* **65,** 175–196.

Simpson, J. H., Gong, W. K. & Ong, J. E. 1997 The determination of the net fluxes from a mangrove estuary system. *Estuaries* **20,** 103–109.

Stigebrandt, A. 1980 Some aspects of tidal interactions with fjords constrictions. *Estuarine, Coastal and Shelf Science* **11,** 151–166.

Turrell, W. R., Brown, J. & Simpson, J. H. 1996 Salt intrusion and secondary flow in a shallow, well-mixed estuary. *Estuarine, Coastal and Shelf Science* **42,** 153–170.

UNESCO 1978 Eighth report of the joint panel on oceanographic tables and standards. *UNESCO Technical Papers in Marine Sciences* No. 28. UNESCO, Paris.

Van de Kreek, J. 1990 Can multiple inlets be stable? *Estuarine, Coastal and Shelf Science* **30,** 261–273.

Vance, D. J., Haywood, M. D. E. & Staples, D. J. 1990 Use of a mangrove estuary as a nursery area by postlarval and juvenile banana prawns, *Penaeus merguiensis* de Man, in northern Australia. *Estuarine, Coastal and Shelf Science* **31,** 689–701.

Wattayakorn, G., Wolanski, E. & Kjerfve, B. 1990 Mixing, trapping and outwelling in the Klong Ngao mangrove swamp, Thailand. *Estuarine, Coastal and Shelf Science* **31,** 667–688.

Wolanski, E., Jones, M. & Bunt, J. S. 1980 Hydrodynamics of a tidal creek–mangrove swamp system. *Australian Journal of Marine Freshwater Research* **31,** 431–450.

Wolanski, E. & Ridd, P. 1986 Tidal mixing and trapping in mangrove swamps. *Estuarine, Coastal and Shelf Science* **23,** 759–771.

Wolanski, E., Mazda, Y., King, B. & Gay, S. 1990 Dynamics, flushing and trapping in Hinchinbrook Channel, a Giant Mangrove Swamp, Australia. *Estuarine, Coastal and Shelf Science* **31,** 555–579.

Wolanski, E., Mazda, Y. & Ridd, P. 1992 Mangrove hydrodynamics. In *Tropical Mangrove Ecosystem.* American Geophysical Union, Washington, DC, 43–62.